

# Carbon nanotubes grown by plasma enhanced chemical vapor deposition of acetylene in the presence of water vapor

## Nanotubos de carbono crecidos con técnicas de deposición química en fase vapor de acetileno asistido por plasma en presencia de vapor de agua

Júlia Sancho-Tàpia <sup>1a</sup>, Enric Bertran-Serra <sup>1b</sup>, Rogelio Ospina-Ospina <sup>1c, 2</sup>

<sup>1</sup> Grupo de investigación ENPHOCAMAT, Departamento de Física Aplicada, Universidad de Barcelona, España. Orcid: [0000-0002-9694-3729](https://orcid.org/0000-0002-9694-3729) <sup>b</sup>, [0000-0002-7392-8059](https://orcid.org/0000-0002-7392-8059) <sup>c</sup>. Emails: [julia.st3110@gmail.com](mailto:julia.st3110@gmail.com) <sup>a</sup>, [ebertran@ub.edu](mailto:ebertran@ub.edu) <sup>b</sup>, [rospinao@ub.edu](mailto:rospinao@ub.edu) <sup>c</sup>.

<sup>2</sup> Grupo Ciencia de Materiales Biológicos y Semiconductores-CIMBIOS, Escuela de Física, Universidad Industrial de Santander, Colombia.

Received: 29 July 2023. Accepted: 30 October 2023. Final version: 6 January 2024.

### Abstract

Carbon nanotubes can be synthesized using various techniques. This work aims to study the experimental process of growing carbon nanotubes via plasma-enhanced chemical vapor deposition (PECVD). Additionally, the study aims to calibrate the reactor and develop a LabVIEW code to introduce water into the process, enabling a water-assisted PECVD procedure. The obtained samples are evaluated through the analysis of SEM images and Raman spectra.

**Keywords:** carbon nanotubes; plasma-enhanced chemical vapor deposition; water-assisted PECVD.

### Resumen

Los nanotubos de carbono pueden ser sintetizados utilizando diversas técnicas. Este trabajo tiene como objetivo estudiar el proceso experimental de crecimiento de nanotubos de carbono mediante deposición química en fase vapor asistida por plasma (PECVD, por sus siglas en inglés). Además, el estudio pretende calibrar el reactor y desarrollar un código en LabVIEW para introducir agua en el proceso, permitiendo así un procedimiento PECVD asistido por agua. Las muestras obtenidas son evaluadas a través del análisis de imágenes SEM y espectros Raman.

**Palabras clave:** nanotubos de carbono; deposición química en fase vapor asistida por plasma; deposición química en fase vapor asistida por plasma y vapor de agua.

### 1. Introduction

Carbon nanotubes (CNTs) are tubular nanostructures made of carbon, they are equivalent to a 2D graphene

layer rolled into a tube [1]. Carbon can form many allotropes, which are structurally different forms of the same elements, such as diamond, graphite, graphene, fullerene, and CNTs. Among them, CNTs stand out as

ISSN Online: 2145 - 8456

This work is licensed under a Creative Commons Attribution-NoDerivatives 4.0 License. [CC BY-ND 4.0](https://creativecommons.org/licenses/by-nd/4.0/)



How to cite: J. Sancho-Tàpia, E. Bertran-Serra, R. Ospina-Ospina, "Carbon nanotubes grown by plasma enhanced chemical vapor deposition of acetylene in the presence of water vapor," *Rev. UIS Ing.*, vol. 23, no. 1, pp. 39-46, 2024, doi: <https://doi.org/10.18273/revuin.v23n1-2024004>

structures with significant potential applications due to their extraordinary physical, mechanical, optical, chemical, and electronic properties [2], [3], [4]. The rapid charge and discharge rates enabled by CNTs make them particularly suitable for the development of batteries and supercapacitor applications [5].

Depending on the number of walls, CNTs can be classified as multiple-walled CNTs (MWCNTs) and single-walled CNTs (SWCNTs).

### 1.1. Conservative Power Theory (CPT)

We will focus on carbon nanotube growth procedures that involve vapor phase synthesis (bottom-up approach), specifically physical vapor deposition (PVD) and chemical vapor deposition (CVD) techniques [6]. PVD techniques involve vaporizing carbon from a solid target through physical processes like arc discharge or laser ablation. On the other hand, CVD techniques utilize a precursor gas that decomposes either by temperature (CVD) or with the assistance of plasma. Once carbon enters the gas phase, the nucleation and growth of carbon structures occur. These structures grow into carbon nanotubes through self-assembly phenomena, sometimes aided by iron nanoparticles and under specific conditions of pressure, temperature, gas mixture, and power [7].

In arc discharge, an electrical discharge is generated between two graphite electrodes to create carbon vapor. This technique was first used by Sumio Iijima in 1991 for the growth of CNTs [1]. On the other hand, laser ablation employs a high-power laser beam focused on a graphite target at high temperatures to vaporize carbon [8].

Nevertheless, the most used technique for CNTs growth is chemical vapor deposition (CVD) due to its scalability for commercial production and the possibility of obtaining long CNTs (Lengths achieved with CVD are around 1mm [9], while lengths measured from PECVD are between 6 to 8  $\mu\text{m}$ ) [10]. The CVD process consists in introducing a hydrocarbon gas, such as  $\text{CH}_4$  into a tubular reactor. The precursor gas entering the reactor decomposes at a high temperature giving rise to different  $\text{CH}_x$  reactive species. The precursor species in contact with the pure Fe nanoparticles (catalyst) donate the carbon atoms that dissolve in the Fe until supersaturation [10]. The carbon is then segregated from the catalyst nanoparticles and arranged in an orderly fashion around the nanoparticle to form the carbon nanotube.

Although these techniques enable the growth of high-quality CNTs, they require high temperatures. One variation of CVD process is plasma-enhanced chemical vapor deposition (PECVD). PECVD operates at lower

temperatures than CVD because the decomposition of the precursor is assisted by plasma. This technique is particularly beneficial for substrates that are sensitive to high temperatures [11].

In the PECVD process, the substrate is prepared with a thin film catalyst, such as Fe. This film is deposited using magnetron sputtering, employing a Fe target located on the cathode [5]. In this technique, a noble gas, typically argon, is introduced into the chamber. A radio frequency (RF) source generates an intense electric field, resulting in the ionization of argon gas and the formation of a plasma state [12]. The electrons in the plasma are confined by the magnetic field near the target (magnetron), causing the ionization of neutrals in proximity to the target. The argon ions, carrying a positive charge, are attracted to the cathode with energies ranging between 100 and 300 eV. As a result, they sputter atoms from the target surface. These sputtered atoms, primarily in the neutral state, are then projected onto the substrate (anode), where the thin film is deposited.

Once the thin film of the catalyst is deposited, an annealing process is carried out. The sample is heated to 730°C. At the nanoscale, the fusion temperature of Fe nanoparticles is lower than bulk Fe, causing the thin film of iron to melt and nucleate in particles. Then, acetylene ( $\text{C}_2\text{H}_2$ ) is introduced and by applying RF, plasma is generated once again, dissociating the gas molecules, and depositing them onto the substrate [17].

### 1.2. Growth mechanism

The growth mechanism of CNTs is explained by the vapor-solid-solid process (VSS) [13], [14]. Firstly, it is necessary to form nanoparticles on the substrate by annealing the thin metallic film of Fe (catalyst). Subsequently, the hydrocarbon gas is decomposed thanks to plasma, releasing hydrogen (H) and carbon (C). The carbon is adsorbed and solved into the Fe nanoparticle. During the process, the concentration of carbon in the nanoparticles increases until supersaturation. Then carbon precipitates on the substrate and the growth of the nanotube is initiated. Carbon nanotube caps are formed around the catalyst nanoparticle, hence the diameter of the CNTs is determined by the diameter of the particle. Moreover, the size of the catalyst nanoparticle, also dictates if SWCNTs or MWCNTs are grown [14]. The growth of CNTs ends when the catalyst loses its activity, which happens when the diffusion of new carbon atoms into the nanoparticle becomes impossible [5].

Based on the interaction between the metallic particle and the substrate, two distinct mechanisms can be distinguished. Firstly, there is the base or root-growth,

characterized by a strong interaction that prevents the metallic particle from separating from the substrate [15]. Consequently, CNTs grow vertically upwards from the particle. On the other hand, there is tip-growth, where the interaction is weaker, causing the metallic particles to detach from the substrate and to be pushed upward, resulting in the formation of CNT structures below them.

### 1.3. Water-assisted PECVD

Some studies have proved significant advantages in using water-assisted chemical vapor deposition (WACVD) for the growth of carbon nanotubes [16]. This is attributed to the inclusion of a small amount of oxidizer, such as  $H_2O$ ,  $O_2$ , or  $CO_2$ , which enhances the growth rate of nanotubes. The presence of these oxidizers leads to the production of hydroxyl (OH) groups, which effectively clean the catalyst particles by removing amorphous carbon and rendering them active for continuous growth.

In this particular study, modifications were made to the PECVD reactor, and a calibration process was conducted to be able to grow carbon nanotubes using water as an additive.

## 2. Experimental procedure

### 2.1. Experimental process for PECVD

The reactor used is a cylindrical chamber constructed from stainless steel [5]. It is equipped with a rotating platform that facilitates the sample movement across different reactor heads (Fig. 1). The two primary heads of the reactor are the sputtering head and the PECVD head. While the reactor can achieve a high vacuum level of  $5 \cdot 10^{-5}$  Pa, the PECVD process is conducted under low vacuum conditions ranging from 2 to 100 Pa. This allows the presence of particles in the chamber for nanoparticle formation and sputtering and plasma processes.

The instrumentation of the system comprises several components, including vacuum gauges (Piranni, Penning and capacitive), vacuum pumps (turbomolecular and mechanic pumps), mass flow controllers, manual and automatic gates, a sample-loading system (load-lock), a pyrometer, a heating system, and an RF-power supply.

The experimental process can be summarized in five steps. Firstly, the Stainless-Steel substrate (SS310) underwent cleaning using either ultrasounds or acetone. Once the sample was cleaned, it was introduced into the reactor chamber using the load-lock system. This system consists of a pre-chamber separated from the main reactor chamber by a gate. Initially, the sample is placed

in the pre-chamber, and the vacuum is established. Subsequently, the gate is opened, allowing the sample to be introduced into the main chamber.

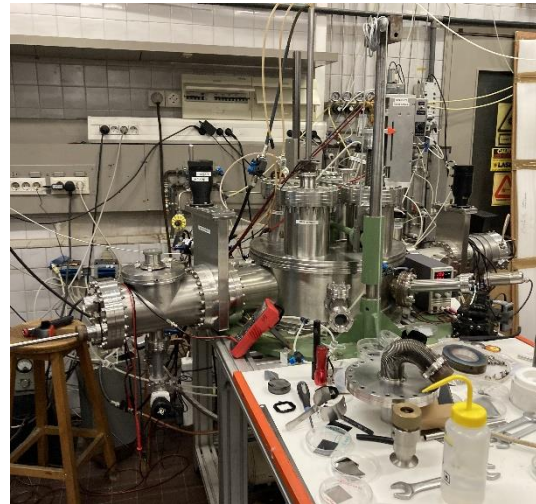


Figure 1. Reactor used to perform the PECVD process.  
Source: own elaboration.

With the sample inside the reactor, the third step involved rotating it towards the sputtering head. The sputtering process, as described in the Production Techniques subsection, was then executed. Argon gas (95sccm) was introduced, creating a plasma. This process lasted for 75 s at a pressure of 2.25 Pa. Once a thin film of iron was deposited onto the substrate, the sample was further rotated to the PECVD head. In this position, the sample was isolated, and an electrode was connected below it to initiate the annealing process. The heating system consisted of a graphite resistance positioned above the substrate and connected to a DC power supply. To monitor the temperature of the sample, an optical pyrometer was employed, and a feedback loop was established with the DC power supply using a proportional-integrative-derivative (PID) controller. During the annealing process, the sample was heated up to  $730^{\circ}C$  following a ramp for 750 s in a reduced atmosphere of hydrogen (100 sccm of  $H_2$ ) at a pressure of 200 Pa. The introduction of hydrogen prevented the oxidation of iron (Fe).

Finally, after 120 seconds, when the sample was thermalized, acetylene (100 sccm of  $C_2H_2$ ) and ammonia (50 sccm of  $NH_3$ ) were introduced in the reactor. Then the plasma was created and the PECVD process was initiated. The duration of the PECVD process can range from 10 min to 1 hour, depending on the desired results. The optimal times to achieve the highest length were 1800 s and 1200 s. However, as in this study we are just

checking CNTs quality the time of the process was not a relevant variable.

The entire process was controlled by a LabVIEW program where some parameters, such as time, could be changed by the user.

In this study, the samples were analyzed by Scanning Electron Microscopy (SEM) (JEOL JSM-7001 F, operated at 20 kV) and Raman spectroscopy ((HR800, Lab-Ram; HORIBA France SAS, Palaiseau, France) with a 532 nm solid-state laser (laser power = 5 mW; diameter =  $\sim 1 \mu\text{m}$ ).

## 2.2. Calibration and changes for WA-PECVD

To be able to perform water assisted plasma enhanced vapor deposition (WAPECVD) some modifications were made to the reactor. A test tube filled with water was connected to the main gas inlet of the reactor (Fig. 2). The water flow through this entrance was regulated by three elements: a microvalve that could be manually adjusted, and two gas valves controlled by alternative opening of the two valves and in previously established periods, commanded by the LabVIEW software.

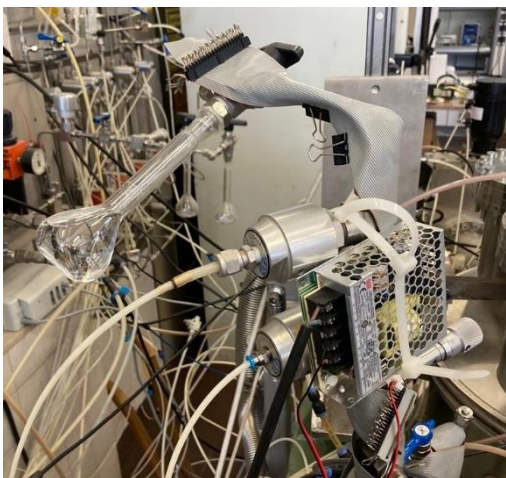


Figure 2. Water test tube, with the heating system and the three gas valves. Source: own elaboration.

A heating system was also installed around the water test tube to prevent water condensation on the walls of the entrance pipe.

Once the physical system was established, it became necessary to automate the flow of water vapor entering the reactor. The aim was to ensure that the water was not introduced all at once, but rather in controlled pulses within specific time intervals. To achieve this pulsating

water flow, a LabVIEW code was developed and integrated into the main code. As a result, water vapor was added in continuous pulses at the same time as  $C_2H_2$  and  $NH_3$  were introduced and until the end of the PECVD process.

In addition, it was necessary to calibrate the amount of water vapor entering the reactor. The theory indicated that the quantity of vapor water needed was 3000 times less than the amount of ammonia  $NH_3$ . Given that the flux of ammonia was 50 sccm ( $cm^3/\text{min}$ ) and knowing that the volume of the reactor is  $V = 60\text{l}$  some calculations were performed resulting in an average mass flow in the order of  $1/60$  sccm. And it was possible to determine that the pressure variation needed to achieve this water ammonia ratio had to be of  $\Delta p = 3\text{Pa}$ . Consequently, the timing between water pulses was adjusted and monitored by the capacitance gauge in order to achieve this specific pressure variation. As a result, the optimum period for maintaining pressure stable and avoiding a peak was determined to be 1s.

## 3. Results

The first sample was developed using the PECVD process without the inclusion of water. The deposition process lasted for 1800 s. On the other side, the second sample was produced using the WAPECVD process, with a duration of 1200 s and a water pulse interval of 1 s.

The analyzed samples have different deposition times because initially, a temporal study of the samples was conducted to determine the optimal time to achieve the greatest length of nanotubes. The investigation revealed 1800 seconds as the optimum time. However, during the water processing, the sample processed for 1200 seconds yielded superior results than the sample processed for 1800 seconds, due to some experimental problems with the reactor. This discrepancy was inconsequential as the emphasis was on nanotube quality, irrespective of length considerations.

### 3.1. SEM analysis

The SEM images from Fig.3 were captured perpendicularly to the sample's surface (a,b,d,e) and also with a vertical sample holder to observe their profile (c, f).

The first ones provide a general view of the nanotubes' uniformity and tips. The white points correspond to the tips, the catalyst nanoparticles, which are visible in the general overview as well as in the closer images.

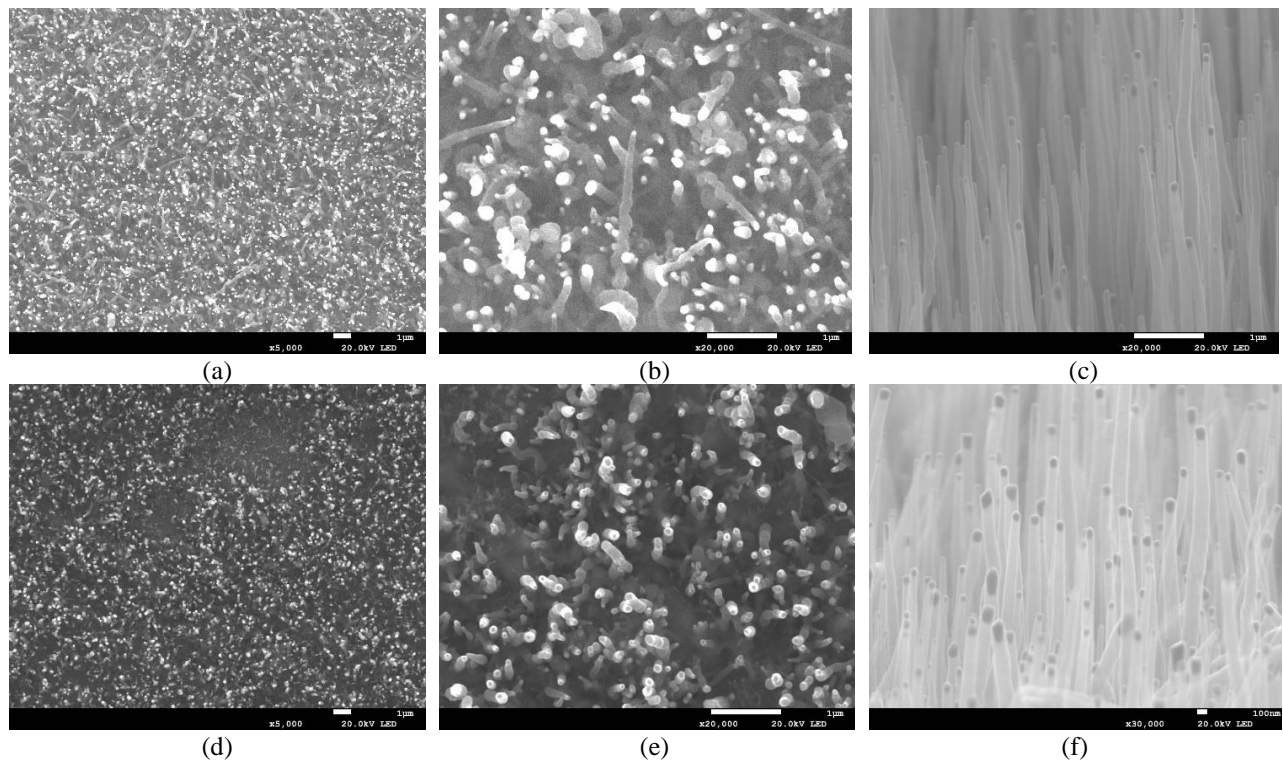


Figure 3. SEM images in different scales for two samples: CNTs by PECVD 1800s (without water): a, b, c. And CNTs by WAPECVD (with water): d, e, f. The first four are perpendicular images (a, b, d, e) and the other two are profile images (c, f). Source: own elaboration. Scale of 1µm for all images but the last one (scale 100nm).

Both sample images indicate a successful growth of carbon nanotubes, hence the water calibration was well-adjusted.

In the profile images (c, f) it is possible to identify better the catalyst particle (Fe) situated on top of the nanotubes. In the WAPECVD image (f), it is evident that the particles are larger, indicating that the growth process was of a shorter duration (1200s). This is independent of the addition of water; it just shows the fact that a shorter process duration consumes less catalyst particles and, therefore results in larger catalyst particles.

On the other side, in the PECVD image (c), the catalyst particles appear smaller, and the nanotubes end in a pointed manner. This means that, as the process lasted longer (1800s) the catalyst was running out and that the nanotube growth became slower.

Furthermore, it was observed that both samples exhibited excellent adhesion properties, as the surface proved to be highly resistant to scratching. In the case of the PECVD sample, the following image (Fig. 4) revealed the presence of an amorphous carbon layer formed between the stainless-steel substrate and the carbon nanotubes.

This layer can be attributed to the deposition of carbon over areas of the substrate where no catalyst particles were present. As a result, the growth of the nanotubes was limited, leading to the formation of numerous short nanotubes and the subsequent development of the amorphous layer.

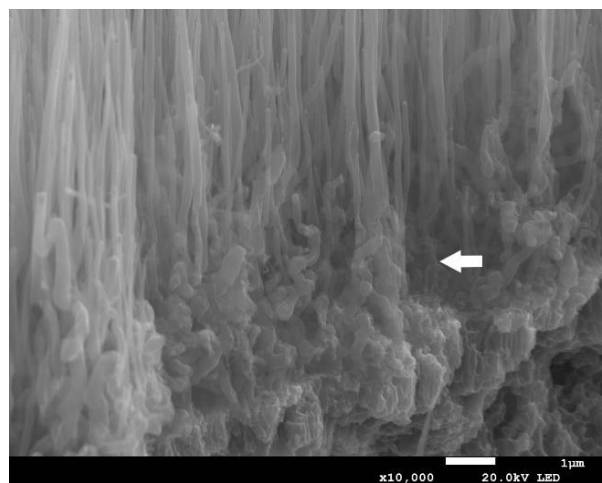


Figure 4. SEM image from the first sample developed through the PECVD process. Source: own elaboration. Scale 1µm.

However, in the WAPECVD sample, the amorphous layer wasn't predominant, suggesting that the application of water vapor had reduced its formation or altered its appearance. This can be explained by the etching power of water vapor [16]. In the first seconds of the process, the amorphous layer is grown in both cases (PECVD and WAPECVD). Yet in the WAPECVD sample, the flux of water vapor etches the amorphous carbon layer, reducing, as well, the defects of the CNTs [18].

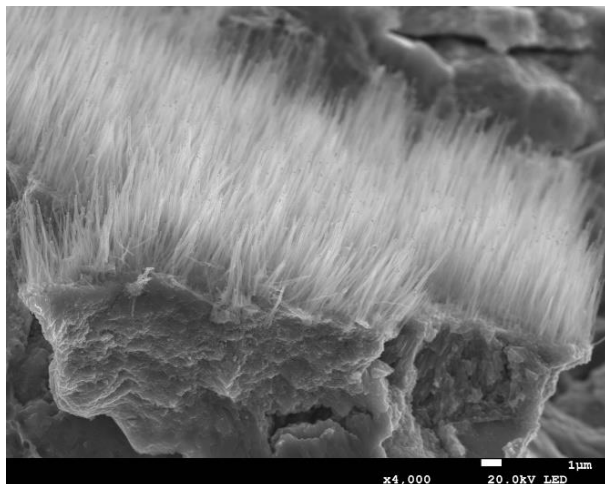


Figure 5. SEM image from the second sample developed through the WA-PECVD process. Source: own elaboration. Scale 1 $\mu$ m.

### 3.2. Raman analysis

The samples were also analyzed by Raman spectroscopy. The resulting spectra (Fig. 6), shows two prominent peaks for each sample. The first peak corresponds to the D-band (1300-1400  $cm^{-1}$ ), also known as the disorder band or defect band, given that it indicates the presence of defects in the structure. The higher the peak, the higher the amount of amorphous carbon in the CNTs. The second peak corresponds to the G-band (1550-1640  $cm^{-1}$ ) which is known as the tangential stretching mode and can be used to determine the layers of the CNTs [19].

By comparing the intensity ratios of these two peaks  $\frac{I_D}{I_G}$ , the quality of the samples can be measured. As we can see in the spectra, the D-band of the water-assisted sample (A) is lower than the D-band of the PECVD sample (B). As a result, the intensity ratio  $I_D/I_G$  decreases from 0.86 to 0.66 for sample B to sample A, suggesting a lower amount of amorphous carbon in sample A. This indicates that the addition of water reduces the amount of amorphous carbon in the CNTs growing process, leading to better quality nanotubes.

Additionally, there is a smaller peak around 2600 -3030  $cm^{-1}$ , which could be attributed to the overlap of two peaks: the 2D band and the G' + D band.

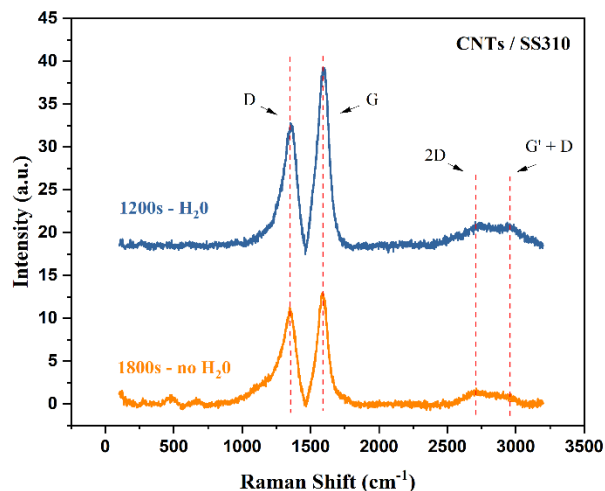


Figure 6. Raman spectra of CNTs grown with water (blue plot) (A) and without (orange plot) (B). Source: own elaboration.

## 4. Conclusions

The conclusions drawn can be summarized as:

- Successful installation and calibration of the pulsed water system that allows the growth of CNTs assisted by water.
- SEM images revealed an amorphous carbon layer between the stainless-steel substrate and CNTs in the PECVD sample. Which was less visible in the WAPECVD sample due to water etching.
- SEM images and Raman spectra analysis indicate that the water-assisted process (WAPECVD) results in the water etching of amorphous carbon layers and an improvement in the quality of the carbon nanotubes with respect of the PECVD process.
- Further studies and optimization of reactor parameters are necessary to explore the potential of water addition in improving the length of the carbon nanotubes during the growth process.

### Funding acquisition

The authors acknowledge financial support from Universidad Industrial de Santander under project 2840-CIIBAEODS 2021, Vice-Rectoría for Research and Extension.

### Autor Contributions

J. Sancho-Tàpia: Conceptualization, Formal Analysis, Investigation, Writing – review & editing. E. Bertran-Serra: Conceptualization, Investigation, Methodology, Validation, Writing – review & editing. R. Ospina-Ospina: Conceptualization, Investigation, Methodology, Validation, Writing – review & editing.

All authors have read and agreed to the published version of the manuscript.

### Conflicts of Interest

The authors declare no conflict of interest.

### Institutional Review Board Statement

Not applicable.

### Informed Consent Statement

Not applicable.

### Acknowledgements

I would like to thank my advisor Dr. Enric Bertran for his dedicated guidance and resources. I would also like to thank Dr. Rogelio Ospina for his assistance in the SEM measurements, Dr. Tariq Jawhari for his assistance with Raman spectroscopy, and Yang Ma for his help in analyzing the spectra.

### References

- [1] S. Iijima, “Helical microtubules of graphitic carbon,” *Nature*, no. 354, pp. 56–58, 1991, doi: <https://doi.org/10.1038/354056a0>
- [2] MF Yu, O Lourie, MJ Dyer, K Moloni, TF Kelly, RS Ruoff, “Strength and breaking mechanism of multiwalled carbon nanotubes under tensile load,” *Science*, no. 287 pp.637–640, 2000, doi: <https://doi.org/10.1126/science.287.5453.637>
- [3] R. Sadri, G. Ahmadi, H. Togun, M. Dahari, S. Newaz Kazi, E. Sadeghinezhad, N. Zubir, “An experimental study on thermal conductivity and viscosity of nanofluids containing carbon nanotubes,” *Nanoscale Research Letters*, vol. 91, 2014, doi: <https://doi.org/10.1186/1556-276X-9-151>

- [4] S. J. Tans, M. H. Devoret, H. Dai, A. Thess, R. E. Smalley, L. J. Geerligs, C. Dekker, “Individual single-wall carbon nanotubes as quantum wires,” *Nature*, vol. 386 pp. 474–477, 1997 doi: <https://doi.org/10.1038/386474a0>
- [5] I. Alshaik, E. Bertran, R. Amade, “Synthesis and Characterization of Carbon nanotubes and Hybrid carbon Nanostructures grown on flexible electrodes for Supercapacitor Applications”, Doctoral dissertation, University of Barcelona, Barcelona, 2021. <http://hdl.handle.net/10803/674294>
- [6] Y. Ando, X. Zhao, T.i Sugai, M. Kumar, “Growing carbon nanotubes,” *Materials Today*, vol. 7, no. 10, pp. 22-29, 2004, doi: [https://doi.org/10.1016/S1369-7021\(04\)00446-8](https://doi.org/10.1016/S1369-7021(04)00446-8)
- [7] M. V. Singh, A. Kumar Tiwari, R. Gupta, “Catalytic Chemical Vapor Deposition Methodology for Carbon Nanotubes Synthesis” *Chemistry Select*, vol. 8, 2023, doi: <https://doi.org/10.1002/slct.202204715>
- [8] T.W. Ebbesen, P.M. Ajayan, “Large-scale synthesis of carbon nanotubes”, *Nature*, 1992. <https://doi.org/10.1038/358220a>
- [9] A. Matyushov “Growth of Carbon Nanotubes Via Chemical Vapor Deposition”, NSF Summer Undergraduate Fellowship in Sensor Technologies.
- [10] S. Hussain, R. Amade, E. Jover, E. Bertran, “Funcionalization of carbon nanotubes by water plasma”, *Nanotechnology*, vol. 23, 2012, doi: <https://doi.org/10.1088/0957-4484/23/38/385604>
- [11] F. Pantoja-Suárez, “Carbon nanotubes grown on stainless steel for supercapacitor applications”, Doctoral dissertation, University of Barcelona, Barcelona, 2019. <https://diposit.ub.edu/dspace/handle/2445/142730>
- [12] C. Bonafos, L. Khomenkhova, F. Gourbilleau, E. Talbot, A. Slaoui, M. Carrada, S. Schamm-Chardon, P. Dimitrakis, P. Normand,” Chapter 7 - Nano-composite MOx materials for NVMs”, *Metal Oxides for Non-volatile Memory*. Elsevier, 2022, doi: <https://doi.org/10.1016/B978-0-12-814629-3.00007-6>
- [13] J. Philippe Tessonier, D. Sheng Su, “Recent Progress on the Growth Mechanism of carbon nanotubes: A Review,” *ChemSusChem*, vol. 4, no. 7, pp. 824-827, 2011, doi: <https://doi.org/10.1002/cssc.201100175>

[14] R. Purohit, K. Purohit, S. Rana, R.S. Rana, V. Patel, "Carbon Nanotubes and Their Growth Methods", *Procedia Materials Science*, vol. 6, Pp. 716-728, 2014, doi: <https://doi.org/10.1016/j.mspro.2014.07.088>

[15] A. Venkataraman, E. V. Amadi, Y. Chen, et al. "Carbon Nanotube Assembly and Integration for Applications," *Nanoscale Res Lett*, vol. 14, 2019, doi: <https://doi.org/10.1186/s11671-019-3046-3>

[16] S. Hussain, R. Amade, E. Bertran, "Study of CNTs structural evolution during water assisted growth and transfer methodology for electrochemical applications," *Materials Chemistry and Physics*, vol. 148, no. 3, pp. 914-922, 2014, doi: <https://doi.org/10.1016/j.matchemphys.2014.08.070>

[17] J. Schäfer, K. Fricke, F. Míka, Z. Pokorná, L. Zajíčková, R. Foest, "Liquid assisted plasma enhanced chemical vapour deposition with a non-thermal plasma jet at atmospheric pressure," *Thin Solid Films*, vol. 630, pp. 71-78, 2017, doi: <https://doi.org/10.1016/j.tsf.2016.09.022>

[18] S. Costa, E. Borowiak-Palen, M. Kruszynska, A. Bachmatiuk, R. Kalenczuk, "Characterization of carbon nanotubes by Raman spectroscopy," *Materials Science-Poland*, vol. 26, no. 2, pp. 433-440, 2008.

[19] A. Ferrari, "Raman spectroscopy of graphene and graphite: Disorder, electron-phonon coupling, doping and nonadiabatic effects," *Solid State Communications*, vol. 143, pp. 47-57, 2007, doi: <https://doi.org/10.1016/j.ssc.2007.03.052>